Nanotherapeutic targeting of the Fn14 receptor for TNBC brain metastases

Christine Carney[1,2], Anshika Kapur[1,2], Pavlos Anastasiadis[1,2], Chixiang Chen[1,2], Graeme Woodworth[1,2], Jeffrey Winkles[2,3,4], Anthony Kim[1,2,5,6]

[1]Department of Neurosurgery, [2]Marlene and Stewart Greenebaum Comprehensive Cancer Center, [3]Department of Surgery, [4]Center for Vascular and Inflammatory Diseases, and [5]Department of Pharmacology, University of Maryland School of Medicine, Baltimore, MD, 21201,[6]Department of Pharmaceutical Sciences, University of Maryland School of Pharmacy, Baltimore, MD, 21201, USA

INTRODUCTION

Despite dramatic improvements in the treatment of most breast cancer subtypes, there are few targeted therapeutics available for treating triple negative breast cancer (TNBC). Even fewer treatment options exist for TNBC that has metastasized to the brain. Advanced drug-loaded nanoparticles (NPs) offer the potential to improve the therapeutic efficacy and pharmacokinetic profile of drugs through use of passive and active targeting. Our group has previously formulated therapeutic 'DART' NPs (**Fig. 1A**) with decreased non-specific adhesivity to extracellular matrix components and phagocytes while retaining targeting to the Fn14 cell surface receptor, which is overexpressed in over a dozen solid cancers, including TNBC metastases. Importantly, we have demonstrated that paclitaxel-loaded DARTs significantly outperform non-targeted NPs and Abraxane, an FDA-approved paclitaxel nanoformulation, in intracranial models of TNBC brain metastasis[1] (**Fig. 1B**). The purpose of this project is to increase our understanding of Fn14 expression by tumor cells and major immune populations within TNBC brain tumor (BT) models and the impact of Fn14 targeting on NP tissue and cellular biodistribution.

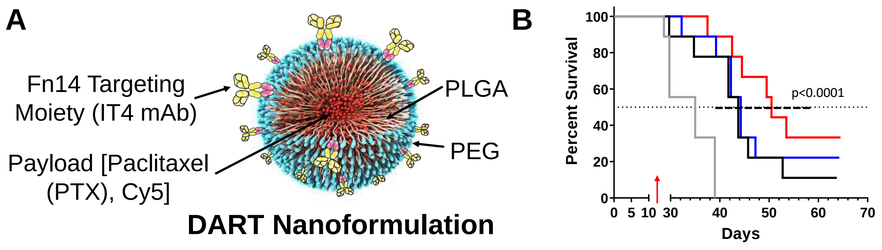

Fig. 1. Schematic and anti-tumor efficacy of DART NPs. (A) DARTs consist of poly(lactic-co-glycolic acid) (PLGA) polymers with a surface coating of polyethylene glycol (PEG) conjugated to IT4, an Fn14 monoclonal antibody (mAb). **(B)** Cumulative Kaplan-Meier survival curve of mice harboring intracranial 231-Br6-Luc tumors after i.v. treatment with saline (grey), Abraxane (black), PLGA-PEG-IgG-PTX (blue), or PLGA-PEG-ITEM4-PTX (red) (10 mg/kg PTX each)[1]

RESULTS

I. Formulation and characterization of Cy5-labeled DART NPs (Cy5-PP-IT4), non-targeted NPs (Cy5-PP-IgG), and Abraxane (Cy5-Abraxane)

Table 1. Physiochemical characteristics of Cy5-labeled NPs.

Formulation	Hydrodynamic diameter (nm)[a]	ζ-potential (mV)[b]	PDI[c]
Cy5-PP-IT4	95.47 ± 3.20	-2.19 ± 0.68	0.100 ± 0.02
Cy5-PP-IgG	90.25 ± 3.32	-4.11 ± 0.37	0.192 ± 0.01
Cy5-Abraxane	163.4 ± 1.114	-8.39 ± 1.21	0.198 ± 0.02

[a]Hydrodynamic diameter measured by dynamic light scattering (DLS)
[b]Surface charge measured at 25°C in 15X diluted PBS w/ 9mM NaCl, pH 7.4
[c]Polydispersity index (PDI) indicates the degree of NP size uniformity measured by DLS

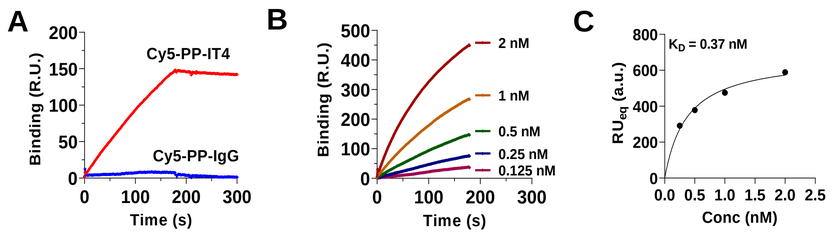

Fig. 2. Specific binding of Cy5-NPs to Fn14-coated sensor chip. (**A**) Surface plasmon resonance (SPR) binding analysis of Cy5-PP-IT4 or Cy5-PP-IgG NPs to a Fn14-coated Biacore chip. (**B**) SPR binding analysis of various concentrations of Cy5-PP-IT4 NPs to a Fn14-coated Biacore chip (relative units, R.U.). (**C**) Binding isotherms of Cy5-PP-IT4 NPs in B were fit by nonlinear regression and used to determine the dissociation constant (K_D).

II. Fn14 is expressed by human MDA-MB-231-TD (231-TD) and murine 66.1-luc TNBC cell lines used in brain tumor (BT) models and enables preferential uptake of targeted NPs *in vitro*

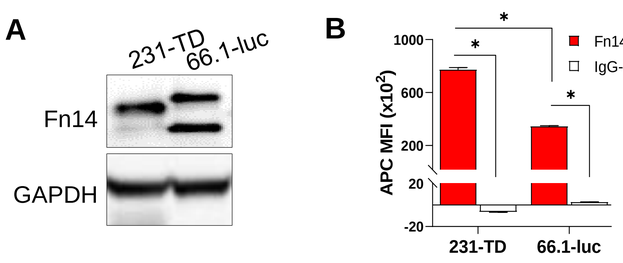

Fig. 3. Fn14 is expressed by human and murine TNBC cell lines, the latter of which also express a splice variant lacking the Fn14 extracellular domain. (**A**) Western blot analysis of Fn14 and GAPDH protein levels in 231-TD and 66.1-luc cells. Murine full-length Fn14 (top band) exhibits slightly different mobility than human Fn14 on SDS-PAGE gel. (**B**) Flow cytometric (FC) analysis of surface Fn14 expression by TNBC cell lines. Cells were stained with Fn14 or isotype control (IgG) antibody and expression quantified from median fluorescent intensity (MFI).

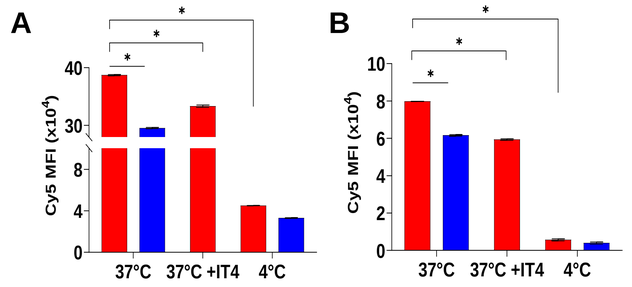

Fig. 4. Cy5-PP-IT4 NPs exhibit preferential uptake by TNBC cells mediated by the Fn14 receptor. FC analysis of Cy5-PP-IT4 (red) and Cy5-PP-IgG (blue) NP uptake in 231-TD (**A**) and 66.1-luc (**B**) cells treated with 25 ug/ml NPs for 30 min either at 37ºC, 4ºC, or after a 30 min pre-incubation with excess IT4 at 37ºC. NP uptake quantified from Cy5 MFI after subtraction of untreated cells. Error bars: mean ± SD, *p<0.0001.

III. Tumor cells are the predominant source of Fn14 expression in the tumor-immune microenvironment (TIME) of xenograft and immunocompetent mouse models of TNBC BTs

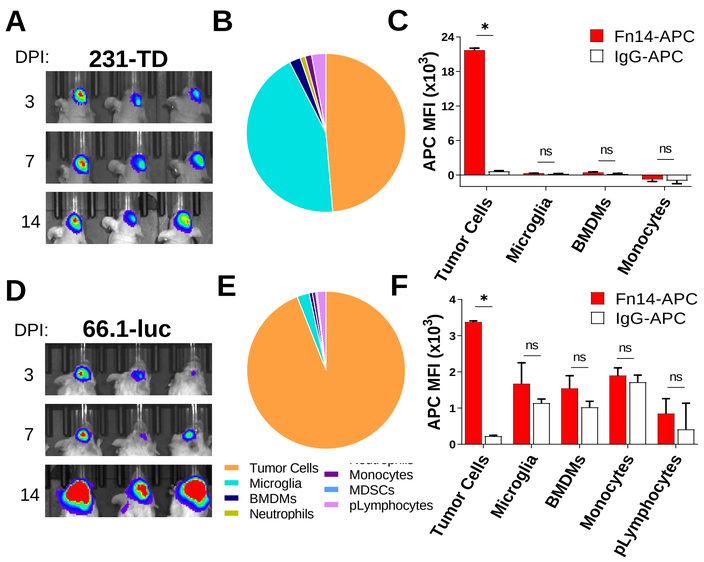

Fig. 5. Tumor cells are the main source of Fn14 expression in xenograft and syngeneic TNBC BT models. Bioluminescent imaging (BLI) of 231-TD (**A**) or 66.1-luc (**D**) BT growth in nude and BALB/c mice, respectively, at the indicated days post inoculation (DPI). (**B, E**) FC analysis of relative frequency of indicated populations in dissociated 231-TD (**B**) and 66.1-luc (**E**) BTs 14 DPI. The following markers were used to identify populations of interest: 231-TD cells (CD45-, GFP+), 66.1-luc (CD45-, luciferase+), Microglia (CD45-int, CD11b+, Ly6C/G-), BMDMs (CD45-hi, CD11b+, Ly6C-lo, Ly6G-), Neutrophils (CD45+, CD11b+, Ly6C-, Ly6G+), Monocytes (CD45+, CD11b+, Ly6C+, Ly6G-), MDSCs (CD45+, CD11b+, Ly6C/G+), pLymphocytes (CD45+, CD11b-). (**C, F**) FC analysis of Fn14 surface expression in indicated populations of dissociated 231-TD (**C**) and 66.1-luc (**F**) BTs. Populations with <3000 events were excluded from analysis. Error bars: +SEM of 4 mice. *p ≤ 0.005, Student's t test. Abbreviations: Bone marrow derived macrophages (BMDMs), myeloid-derived suppressor cells (MDSCs), putative lymphocytes (pLymphocytes).

IV. Fn14 targeting does not promote NP clearance in tumor-naïve mice or increase NP association with tumor-harboring brains

Fig. 6. Cy5-PP-IT4 NPs exhibit similar clearance as Cy5-PP-IgG in tumor-naïve BALBc mice. Analysis of NP clearance after i.v. injection via IVIS *in vivo* fluorescent imaging and quantified as the percent of the initial dose (% ID). Data was fit by non-linear regression analysis using GraphPad software. Asterisks above/below the curves indicate significant differences between Cy5-PP-IT4 and Cy5-Abraxane/Cy5-PP-IgG respectively, *p<0.05.

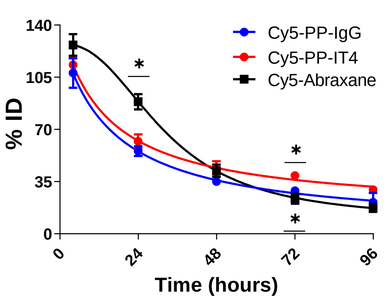

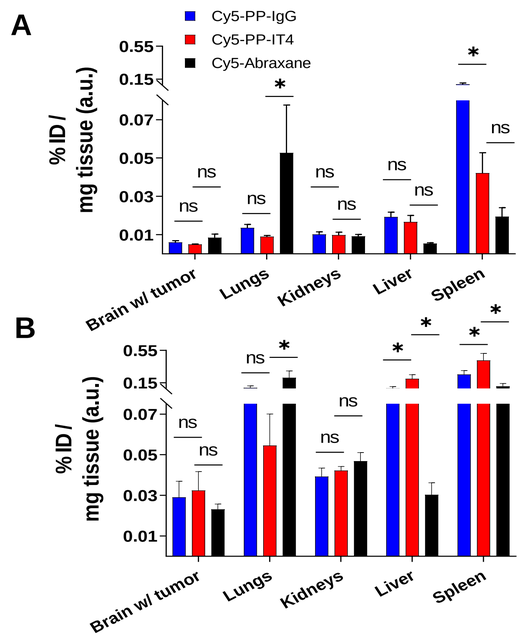

Fig. 7. NP biodistribution in BT-harboring mice reveals Fn14 targeting does not result in increased NP tumor accumulation in brains with tumors 24hr after systemic administration. IVIS *ex vivo* imaging analysis of NP tissue distribution in nude (**A**) and BALBc (**B**) mice harboring 231-TD and 66.1-luc BTs, respectively, 24hr after i.v. injection. Tissue Cy5 signal was quantified as a percent of the Cy5 initial dose (% ID) and normalized to tissue weight (arbitrary units, a.u.). Error bars: +SEM of ≥3 mice, *p<0.01.

V. Fn14 targeting enables significant and specific targeting of Fn14-positive tumor cells in the TIME of xenograft and immunocompetent models of TNBC BT growth

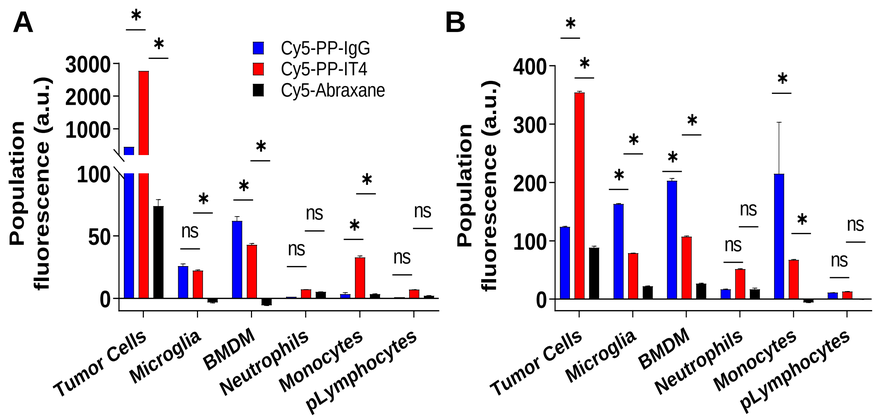

Fig. 8. DART NPs specifically target Fn14-positive tumor cells within BTs. FC analysis of NP cellular targeting in dissociated 231-TD (**A**) and 66.1-luc (**B**) BTs 24hr after IV administration. Population fluorescence indicates Population fluorescence quantified from the population Cy5 MFI normalized by the respective population frequency (arbitrary units, a.u.). Error bars: +SEM of ≥3 mice, *p≤0.0005.

CONCLUSIONS

In this study, we formulated Cy5-labeled DARTs (Cy5-PP-IT4 NPs), non-targeted NPs, and Abraxane (**Table 1**) and first confirmed DART specific binding (**Fig. 2**) via SPR. Next, after assessing Fn14 expression by human 231-TD and murine 66.1-luc TNBC cells via Western blotting and FC (**Fig. 3),** we demonstrated preferential cellular uptake of Cy5-PP-IT4 NPs *in vitro* via FC (**Fig. 4**). We then used these TNBC cells to develop complementary xenograft and immunocompetent TNBC BT models of brain metastasis and found that tumor cells are the predominant source of Fn14 expression in BT TIMEs, with minimal Fn14 expression by microglia, infiltrating macrophages, monocytes, and lymphocytes (**Fig. 5**). In keeping with a systemic delivery strategy, we examined clearance and found that DART NPs exhibit similar extended circulation time and clearance patterns as non-targeted NPs (**Fig. 6**). We next evaluated NP biodistribution in mice harboring TNBC BTs 24 hr after systemic administration and did not see a significant difference in DART vs. non-targeted NP BT accumulation (**Fig. 7**). However, analysis of dissociated TNBC BTs revealed significant, specific targeting of DARTs to Fn14-positive tumor cells in both models (**Fig. 8**). Together, these results provide valuable new data pertaining to the potential efficacy of this drug delivery platform for treating brain-metastatic tumors through Fn14-mediated targeting of NPs to cancer cells residing within the brain TIME.

METHODS & STATISTICAL ANALYSIS:
Methods are described in the figure legends. Statistical analyses were performed via 2-way ANOVA and FDR method of Benjamini and Hochberg for multiple comparisons or as otherwise specified in the figure legends.

REFERENCES:
[1]Dancy JG, *et al.* (2020). *Sci Adv.* 6(3)eaax3931.

FUNDING:
NIH R37 CA218617, NIH RO1 NS108813